JOURNAL OF PROPULSION AND POWER
Vol. 11, No. 1, January–February 1995

Effect of Bleed Configuration on Shock/Laminar Boundary-Layer Interactions

A. Hamed*
University of Cincinnati, Cincinnati, Ohio 45221
and
T. Lehnig†
Cold Jet, Inc., Loveland, Ohio 45140

The flowfield characteristics are simulated numerically in an oblique shock wave/laminar boundary-layer interaction for three different bleed configurations. The numerical solution for the flowfield is obtained for the strong conservation-law form of the two-dimensional compressible Navier-Stokes equations using an implicit scheme. The computations model the flow in the interaction region and inside the bleed slot for an impinging oblique shock of sufficient strength to cause boundary-layer separation on a flat plate boundary layer. The computed results are presented for a normal bleed slot at three different locations: 1) upstream, 2) across, and 3) downstream of the shock impingement point. The detailed flow characteristics in the interaction zone and inside the bleed slot are compared for the three cases. The resulting surface pressure and shear stress and boundary-layer displacement and momentum thickness distributions are also compared for the three bleed cases and for the shock wave/boundary-layer interaction without bleed.

Introduction

AIR bleed systems are used for controlling the shock wave/boundary-layer interactions when operating at supersonic speeds. Proper bleed system design is particularly important for the efficient and stable operation of mixed compression supersonic inlets.[1] The fundamental objectives of supersonic inlet bleed system design are to provide good aerodynamic flow characteristics with minimum boundary-layer bleed.[2,3] The elimination or reduction of separation in shock wave/boundary-layer interactions[4] is essential for controlling the pressure loss and maintaining a stable flowfield in supersonic inlets. Minimizing the bleed required to achieve boundary-layer control allows the penalties associated with incorporation of a supersonic inlet bleed system to be minimized as well. These penalties include a loss of inlet mass flow and an increase in drag due to venting of the bleed air into the freestream. Ideally, removal of only that portion of the low-momentum boundary layer needed to inhibit separation is desired.

Comparisons of internal flow computational results[5–7] with the experimental measurements in supersonic inlets[4,8] revealed reasonable agreement between the computed and measured surface pressures upstream of the ramp bleed. However, discrepancies in the predicted shock locations and velocity profiles were observed downstream of shock/boundary-layer interactions with bleed.

Hamed and Shang[1] reviewed the existing experimental data base for shock wave/boundary-layer interactions in supersonic inlets and other related configurations. According to this survey, there is enough experimental evidence[9–14] to indicate that local bleed can control flow separation in shock wave/boundary-layer interactions. There are disagreements,[1] however, among the different experimental results regarding the effects of bleed hole size,[13,14] and location relative to the shock.[9–12] Strike and Rippy[9] measured the surface pressure in the interaction zone of an oblique shock wave impinging a turbulent boundary layer over a flat plate, with suction. They determined that less suction is required to control separation, when applied upstream of the shock. Seebaugh and Childs[10] investigated experimentally the axisymmetric flow in the interaction region of the boundary layer inside a duct. Contrary to the conclusions of Strike and Rippy,[9] suction within the interaction region was found to be more effective in suppressing the effects of separation.

The purpose of this study is to clarify the effect of bleed location on controlling flow separation in shock wave/boundary-layer interactions. Numerical computations are performed to determine the flow characteristics in the interaction zone of an oblique shock wave/boundary layer, and within a normal bleed slot, upstream, downstream, and across the oblique shock impingement point.

Computational Details

The bleed study is conducted initially for laminar flow, in order to allow the flowfield characterization to be accomplished without the uncertainties associated with turbulence modeling. The partial differential equations used to describe the flow are the time-dependent compressible Navier-Stokes equations in strong conservation law form. The flow is treated as a perfect gas with molecular dynamic viscosity given by Sutherland's law, and a gas conductivity based on a constant Prandtl number. An implicit approximate factorization technique[15] is used in the numerical solution of the governing equations. Prior to the bleed investigation, the code[16,17] has been validated for laminar shock wave/boundary-layer interactions both for separated and unseparated flows[18] by comparing the computational results with Hakkinen's experimental data.[19]

The solution is obtained in a domain that includes the interaction region and the interior of the bleed port as shown schematically in Fig. 1. The specified static pressure at the bottom of the bleed slot simulates the plenum pressure that controls the bleed level for a given slot and flow configuration. Zero-order interpolations are applied for the rest of the flow variables at the bottom of the bleed slot. The no-slip condi-

Presented as Paper 91-2014 at the AIAA/SAE/ASME/ASEE 27th Joint Propulsion Conference, Sacramento, CA, June 24–26, 1991; received Aug. 2, 1991; revision received May 4, 1993; accepted for publication May 9, 1994.

*Professor, Department of Aerospace Engineering and Engineering Mechanics. Fellow AIAA.
†Senior Project Engineer. Member AIAA.

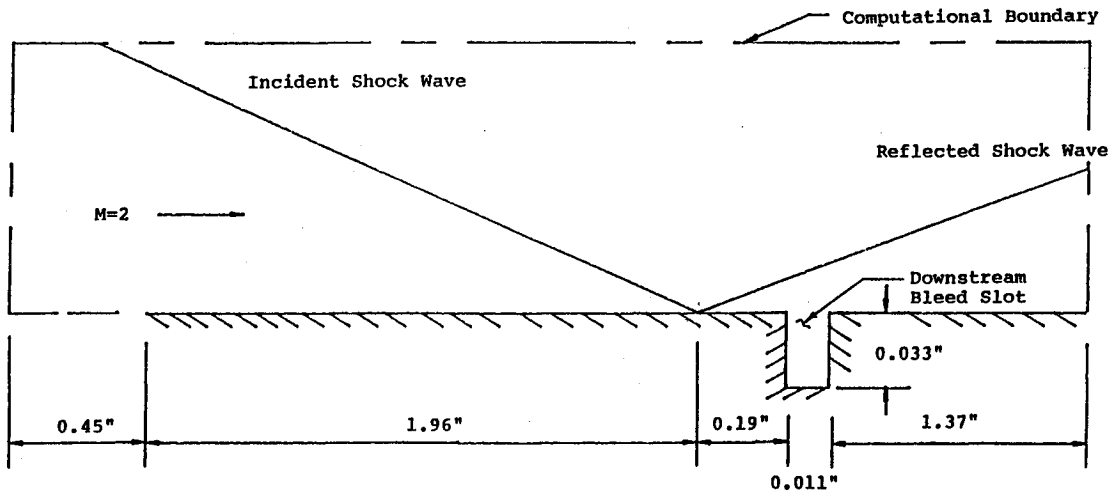

Fig. 1 Schematic of the solution domain for the shock-wave/boundary-layer/bleed interaction.

tion, adiabatic wall, and zero normal pressure gradients are specified at the solid surfaces. The impinging shock wave is explicitly introduced at the upper boundary using the Rankine-Hugoniot relations. Zero-order extrapolation of the flow variables is enforced at the downstream boundary, which is carefully positioned such that all generated or reflected shocks exit through it.

The orthogonal grid spacing was varied in both the streamwise and normal directions to capture the important flow characteristics in the shock wave/boundary-layer interaction zone and inside the bleed slot.[18] The computational grid consisted of (243 × 107) mesh points in the streamwise and normal directions, respectively, with grid clustering at the plate and around the slot walls. The following grid distribution was implemented in the solution of the shock-wave/laminar boundary-layer interactions with bleed:

$$\Delta Y_j = 0.0375 \qquad 77 \le j \le 107 \tag{1}$$

$$\Delta Y_j = 1.125\Delta Y \qquad 36 \ge j \ge 76 \tag{2}$$

$$\Delta Y_j = 1.5625 \times 10^{-4} \qquad 28 \le j \le 35 \tag{3}$$

$$\Delta Y_j = 1.125\Delta Y_{j-1} \qquad 1 \le j \le 27 \tag{4}$$

where $j = 1$ represents the bottom, and $j = 32$ the top of the bleed slot.

The grid inside the bleed slot consisted of (34 × 32) mesh points in the streamwise and normal direction, respectively. Stretching was used in the streamwise direction, in order to cluster the grid points inside, and near the slot as follows:

$$\Delta X_i = 0.03 \qquad i \le I - 64, \qquad I + 63 \le i \tag{5}$$

$$\Delta X_i = 1.5625 \times 10^{-4} \qquad I - 20 \le i \le I - 13 \qquad I + 13 \le i \le I + 20 \tag{6}$$

$$\Delta X_i = 1.125\Delta X_{i+1} \qquad I - 21 \ge i \ge I - 63 \qquad I + 12 \ge i \ge I + 1 \tag{7}$$

$$\Delta X_1 = 1.125\Delta X_{i-1} \qquad I - 12 \le i \le I \qquad I + 21 \le i \le I + 62 \tag{8}$$

where $i = I$ represents the grid at the center of the bleed slot.

The flow solution convergence monitoring was based on the shear stress at the plate surface τ_w, as follows:

$$\varepsilon = \left| \frac{\tau_w^n - \tau_w^{n-1}}{\tau_w^n} \right|$$

The specified convergence criterion was $\varepsilon \le 10^{-4}$ for the evaluation points at $X < X_{sh}$, and $\varepsilon \le 10^{-5}$ for the evaluation points located at $X > X_{sh}$ to account for the different rates for convergence at the different locations from the plate leading edge (where X_{sh} is the tested shock impingement point location).

Results and Discussion

Results are presented for the computed flowfield in the interaction zone of an oblique shock/laminar boundary-layer interaction with bleed applied through a normal slot at three different locations relative to the shock impingement point. The freestream conditions are 2.0 Mach number and 2.96×10^5 Reynolds number, based on the shock impingement location, $x = 1.96$ in., from the flat plate leading edge. The shock angle of 32.585 deg corresponds to the test conditions of Hakkinen et al.[19] for the separated flow case. The computations are performed at the same freestream conditions and shock strength, with bleed applied through a normal slot that is 0.011 in. wide and 0.033 in. deep. The slot width was equal to the boundary-layer displacement thickness before the interaction, and its depth-to-width ratio of 3 is selected based on the experimental results of the optimization study by Syberg and Koncsek.[2] The slot was positioned at three different locations, upstream, downstream, and across the shock impingement point. For across the shock bleed, the slot center was positioned directly at the shock impingement point with the flat plate surface ($X_{sh} = 1.96$ in.). The downstream bleed case was chosen such that the centerline of the bleed slot is at the location of the maximum computed surface shear stress in the separated flow case without bleed ($x = 2.167$ in.). The upstream bleed location was similarly selected at the opposite side relative to the shock impingement point with the centerline at $x = 1.753$ in. from the leading edge. The slot base pressure was maintained at the same value (0.42 of preshock pressure), which resulted in bleed mass rates of 3.42, 4.65, and 5.05% of the upstream boundary-layer mass flow for upstream, across, and downstream bleed cases, respectively. Some of the computed results for downstream bleed configuration were reported earlier.[18] Here, the results of the flowfield computations in the shock/boundary-layer/bleed interaction zone are presented for the upstream and across the shock bleed. The computed results are compared for the three bleed locations and for the case with no bleed.

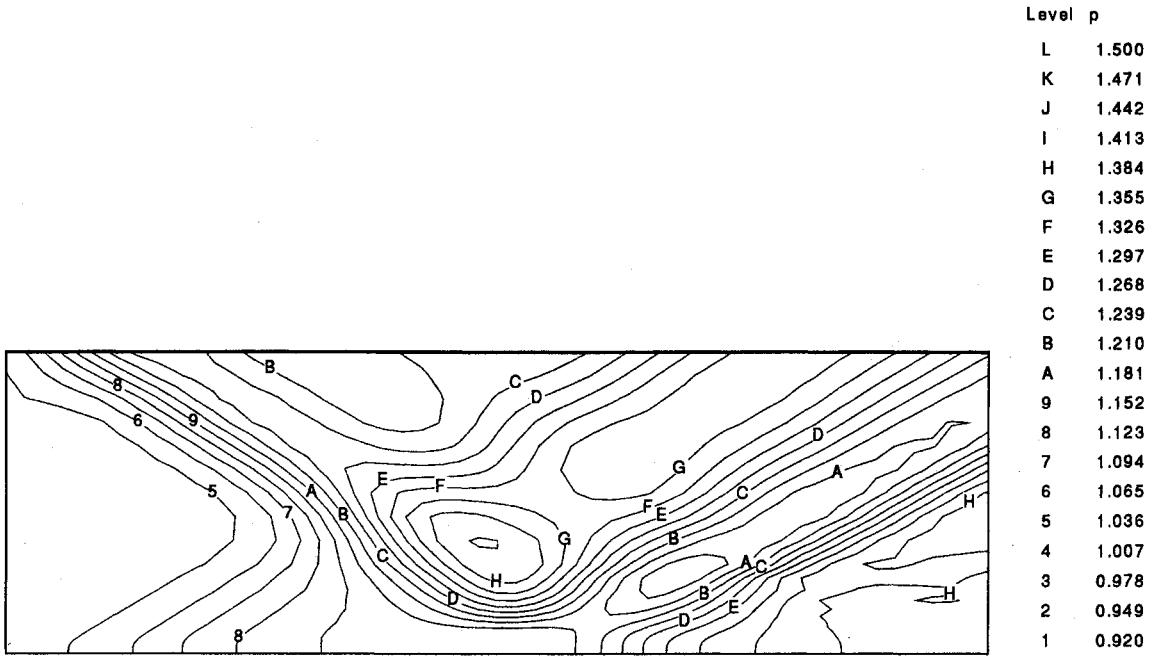

Fig. 2 Pressure contours for the no-bleed case.

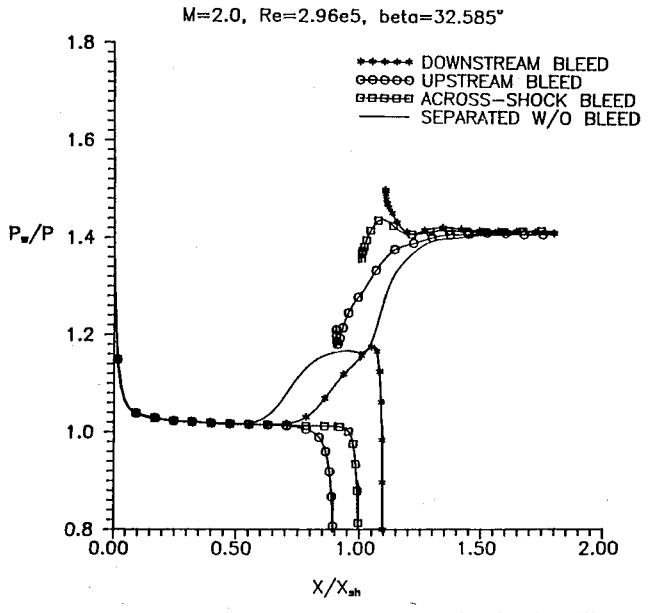

Fig. 3 Comparison of surface pressure distribution for the different bleed configurations.

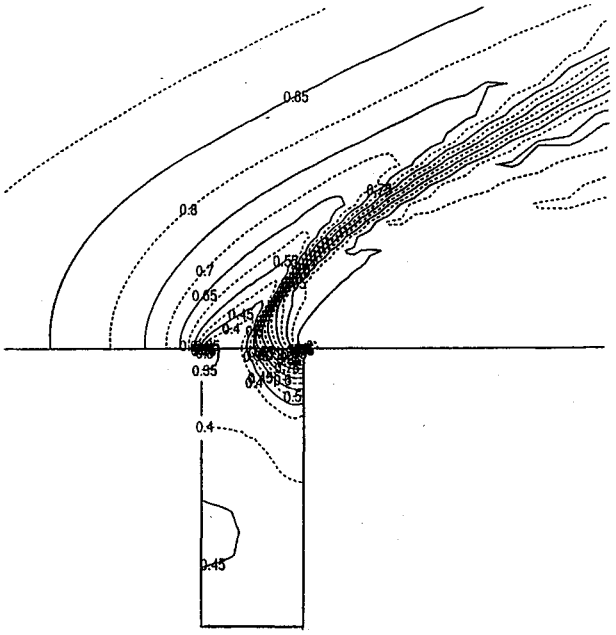

Fig. 4 Pressure contours for upstream bleed.

Figure 2 shows the pressure distribution near the interaction zone for the no bleed case. The incident shock and the separation and reattachment shocks are seen in this figure. Figure 3 shows the plate surface pressure distribution of the three bleed cases and for no bleed. The wall pressure distribution shows a significant reduction in the length of the interaction region compared to the nonbleed case, and an elimination of the pressure plateau in all three bleed configurations. Furthermore, the pressure ratio downstream is slightly increased over the nonbleed interaction case. These observations agree with previous reports on the effect of bleed, as discussed by Hamed and Shang.[1] Figure 3 clearly shows that there is a big difference in the static pressure, at the corner of the flat plate surface and the downstream slot wall for the three bleed cases. This pressure is lowest ($p/p_\infty = 1.22$) for the upstream bleed case, and highest ($p/p_\infty = 1.5$) for the downstream bleed case with the across the shock pressure value in between ($p/p_\infty =$ 1.36). As for the static pressure distribution downstream of the bleed slot, there is an abrupt pressure drop for a short distance followed by a gradual pressure rise in the upstream bleed case. However, in the downstream bleed case, the static pressure over the plate surface drops downstream of the bleed slot, whereas in the across the shock bleed case the pressure rises first, then drops slightly.

One can see that in both the upstream and across the shock bleed cases, the pressure starts to drop before the slot opening and reaches a value of $p/p_\infty \sim 0.8$ at the intersection of the flat plate with the upstream slot wall. In the case of downstream bleed, the pressure initially builds up on the plate surface upstream of the slot opening, reaching a value slightly higher than that of the plateau pressure in the case of separated flow without bleed ($p/p_\infty \sim 1.2$), followed by a very sharp drop to 0.8 at the upstream slot wall corner. In all three cases, there is an initial moderate pressure drop over the first

part of the slot opening followed by a sharp rise across a shock emanating inside the slot as shown for the upstream bleed pressure contours of Fig. 4.

The Mach number contours are presented in Figs. 5–7. The contours indicate a choked flow in all three bleed cases. The subsonic boundary-layer flow entering the bleed slot initially accelerates due to the separation bubble at the upstream wall of the bleed slot that acts as a converging-type constriction. After passing through the convergent section of the constriction, the now choked flow goes through a brief expansion region where the flow is further accelerated. The flow then decelerates towards the slot exit as it reaches an effectively constant area downstream of the separation bubble.

The velocity distributions across the slot opening are shown in Figs. 8–10. Generally the normal velocity component increases gradually across the slot opening and reaches a plateau $v/U_\infty \sim -0.3$ somewhere in the downstream half of the bleed slot, with a slight increase further near the downstream slot wall in the two cases of across the shock and downstream

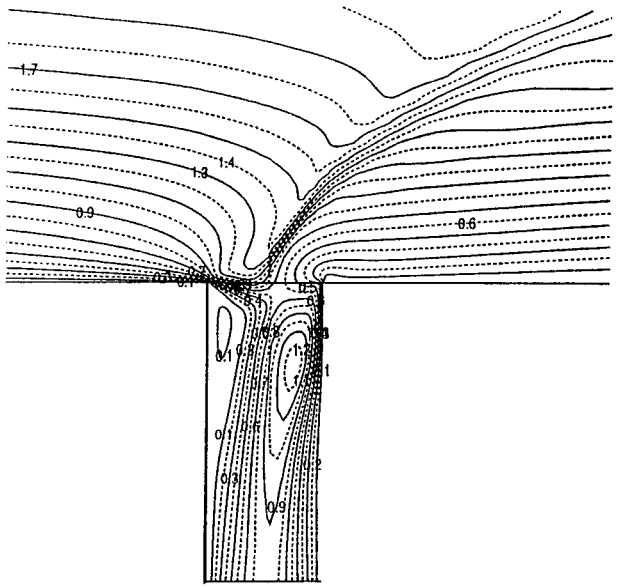

Fig. 5 Mach number contours for upstream bleed.

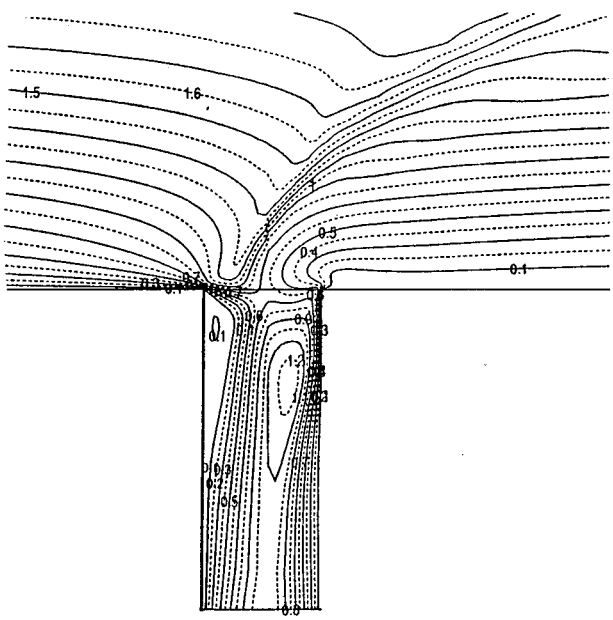

Fig. 6 Mach number contours for across the shock bleed.

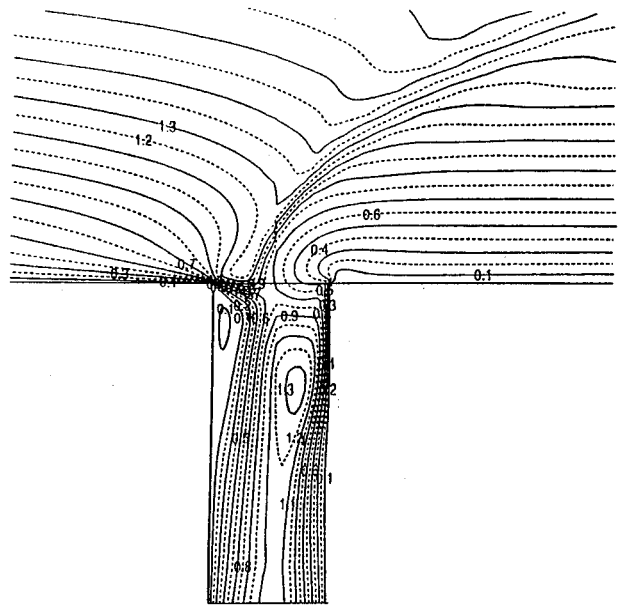

Fig. 7 Mach number contours for downstream bleed.

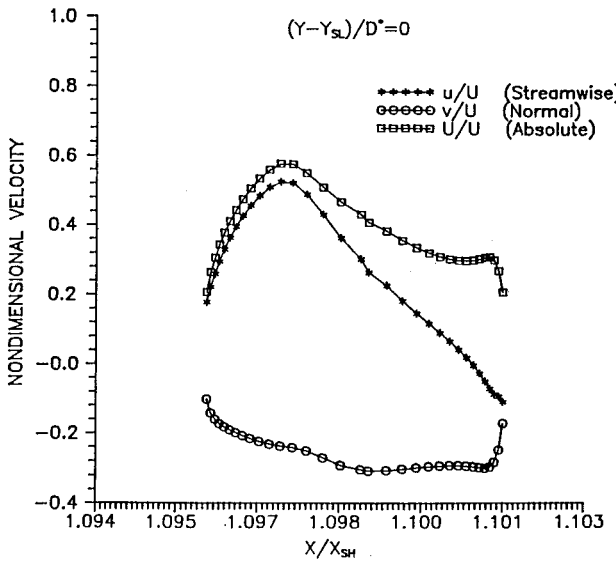

Fig. 8 Velocity distribution across slot opening for upstream bleed.

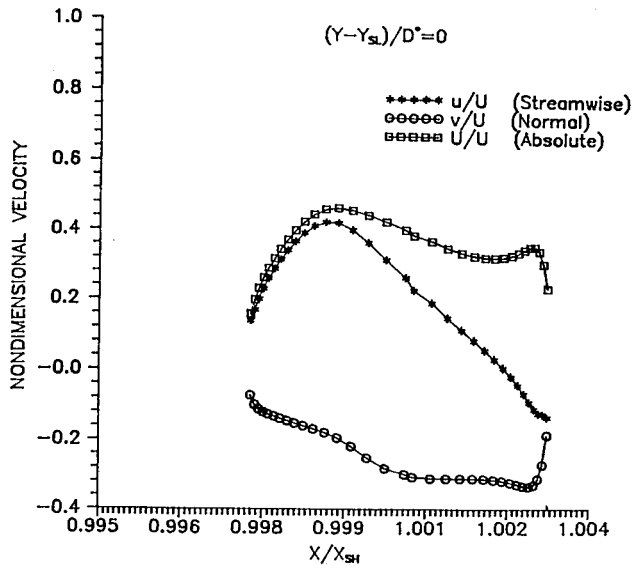

Fig. 9 Velocity distribution across slot opening for across the shock bleed.

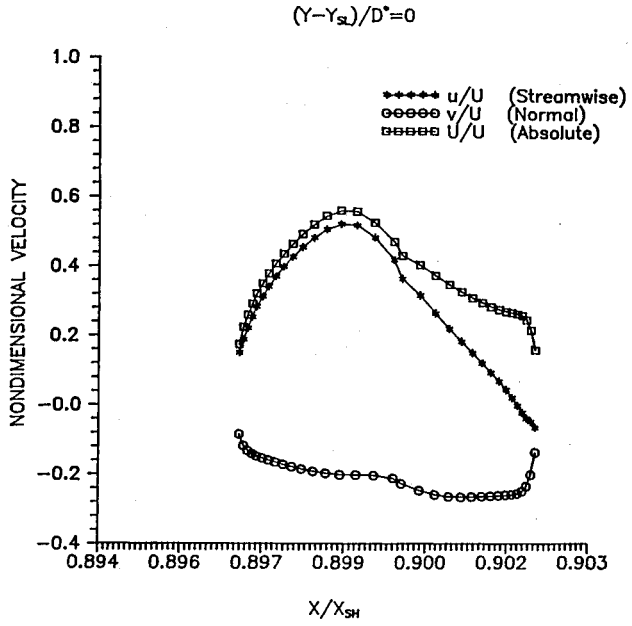

Fig. 10 Velocity distribution across slot opening for downstream bleed.

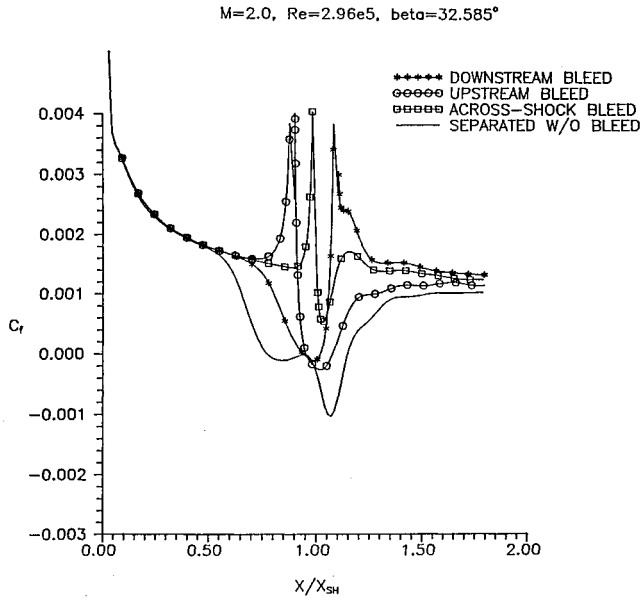

Fig. 11 Comparison of the skin friction coefficients for the different bleed configurations.

bleed. On the other hand, the streamwise velocity component reaches a local u/U_∞ of 0.5–0.6 upstream of the slot shock, then drops linearly reaching slightly negative values (-0.02 to -0.1) near the downstream slot corner. Typically, in the computations of flowfields involving bleed, the bleed mass flux is specified while the tangential velocity is set equal to zero across the bleed zone. The results of Figs. 8–10 suggest that the neglect of the streamwise velocity component in the bleed zone of shock wave/boundary-layer interaction can constitute a serious source of error in the computations. This might be a major cause of discrepancies between the computed and experimental results downstream of the interaction bleed zone in supersonic inlets.[5–7]

Figure 11 presents the computed skin friction distribution over the flat plate surface for the three bleed locations and for the no bleed separated flow case. The reduction in the length of the interaction zone due to bleed is clear in this

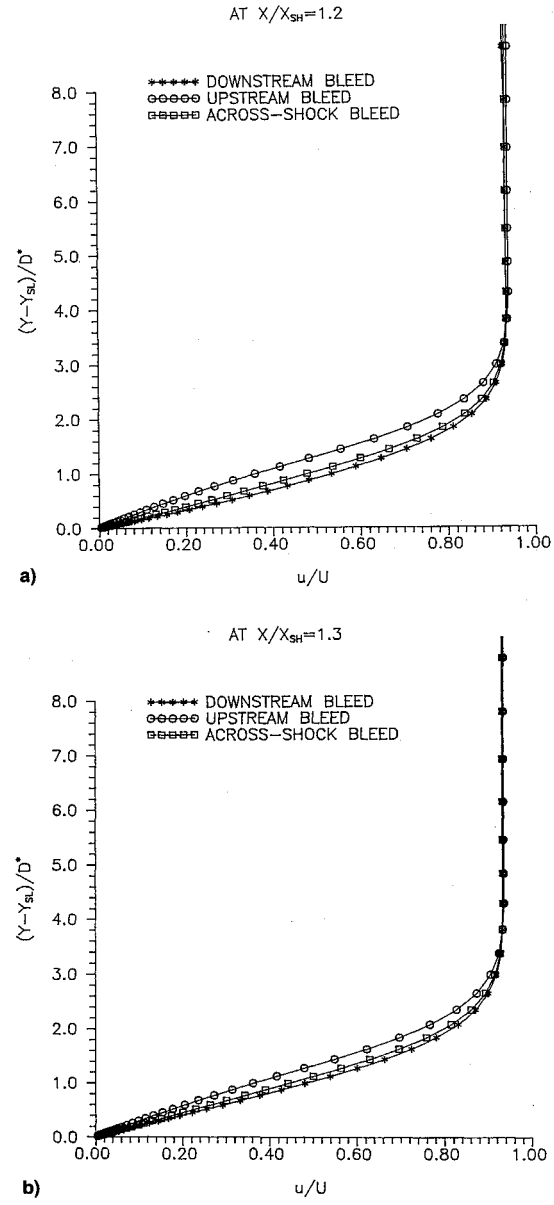

Fig. 12 Comparison of the velocity profiles downstream of the interaction zone for the different bleed configurations.

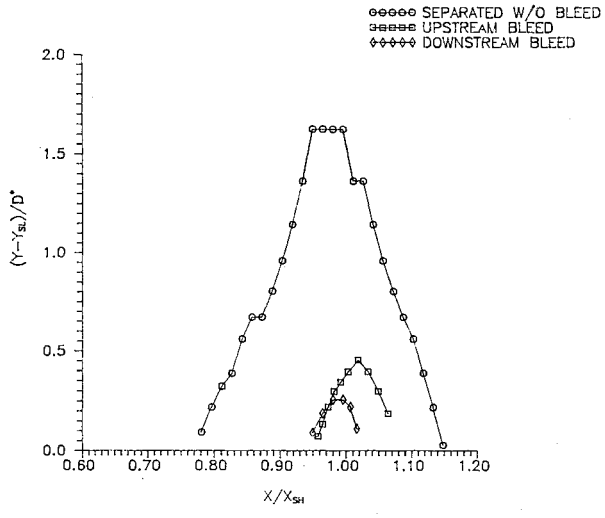

Fig. 13 Comparison of separation region for the different bleed configurations.

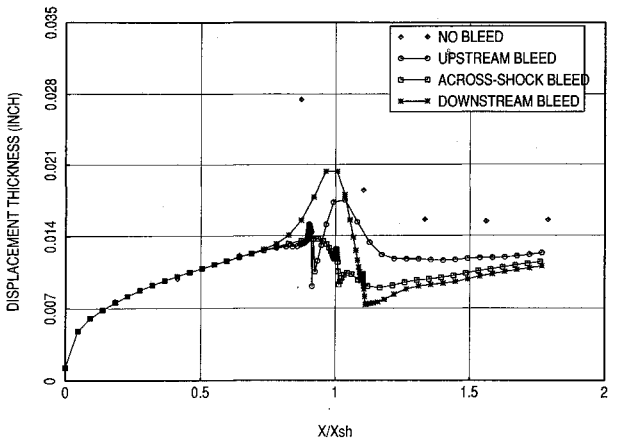

Fig. 14 Comparison of the boundary-layer displacement thickness for the different bleed configurations.

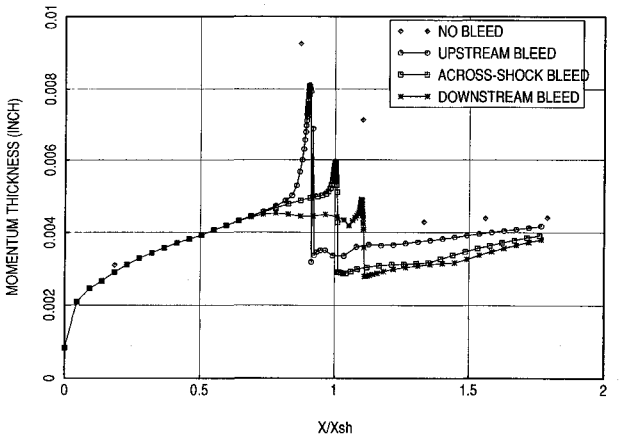

Fig. 15 Comparison of the boundary-layer momentum thickness for the different bleed configurations.

figure for all three cases. However, a small flow separation zone as indicated by the negative skin friction coefficient can be observed for the upstream and downstream bleed cases, but not for across the shock bleed. The friction coefficients are higher for all three bleed cases downstream of the interaction zone in comparison to the no bleed friction, indicating fuller velocity profiles. The highest friction coefficient value downstream of the interaction is for the downstream bleed, and the lowest for the upstream bleed. These differences in the velocity profiles appear to persist for a long distance downstream of the interaction as can be seen in the velocity profiles of Fig. 12.

Figure 13 compares the extent of the separation regions as determined from $u = 0$. One can observe that the separation bubble height is reduced to 32 and 25% of its value without bleed for the cases of upstream and downstream bleeds, respectively. Across the shock bleed completely eliminates separation as indicated by the skin friction results of Figs. 11 and 12. The boundary layer's displacement and momentum thickness are presented for the three bleed locations and for no bleed in Figs. 14 and 15. One can see that the largest reduction in δ^* and θ are realized in the downstream bleed case and the least reduction for upstream bleed.

Conclusions

A numerical investigation was conducted to determine the effect of bleed location on the flow in an oblique shock/boundary-layer interaction. The implicit factored scheme of Beam and Warming[15] was used to obtain numerical solutions of the two-dimensional compressible Navier-Stokes equations in strong conservation law form. The investigation was restricted to laminar flows to avoid the uncertainties associated with turbulence modeling. The solution domain extended inside the normal bleed slot, and computational grid was clustered near the surfaces. Three bleed locations upstream, across, and downstream of the shock impingement point were investigated for the same slot size and static pressure at the bottom of the bleed port. Results were presented for pressure and Mach number throughout the interaction region and inside the bleed port, and for the surface pressure and skin friction distribution. According to the computed results, the across-shock bleed proved to be the most effective in preventing separation and shortening the interaction length, whereas the upstream bleed slot proved to be the least effective. The results indicate that the downstream bleed slot location produced the most favorable velocity profiles and skin friction recovery downstream of the interaction region, as well as the maximum reduction in boundary-layer momentum and displacement thickness. The results suggest that a combination of across-shock and downstream bleed slots might provide the two advantages, namely no flow separation in the interaction region and fuller boundary-layer profiles downstream of the interaction zone.

Acknowledgments

This work was supported by NASA Lewis Research Center Contract NASA NAG3-1213. The computational work was performed on the Cray Y-MP128 of Ohio Supercomputer, Columbus, Ohio.

References

[1]Hamed, A., and Shang, J., "Survey and Assessment of the Validation Data Base for Shock Wave Boundary Layer Interactions in Supersonic Inlets," AIAA Paper 89-2939, July 1989.

[2]Syberg, J., and Koncsek, J. L., "Bleed System Design Technology for Supersonic Inlets," AIAA Paper 72-1138, Nov./Dec. 1972.

[3]Fukuda, M. K., Hingst, W. R., and Reshotko, E., "Bleed Effects on Shock/Boundary-Layer Interactions in Supersonic Mixed Compression Inlets," *Journal of Aircraft*, Vol. 14, No. 2, 1977, pp. 151–156.

[4]Hamed, A., "Flow Separation in Shock Wave-Bounday Layer Interactions at Hypersonic Speeds," NASA CR 4274, Feb. 1990.

[5]Martin, A. W., Koslin, L. C., and Sidney, D. M., "Dynamic Distortion at the Exit of a Subsonic Diffuser of a Mixed Compression Inlet," NASA CR-1644, Dec. 1970.

[6]Knight, D. D., "Improved Calculation of High Speed Inlet Flows. Part I: Numerical Algorithm," *AIAA Journal*, Vol. 19, No. 1, 1981, pp. 34–41; also see "Part II: Results," *AIAA Journal*, Vol. 19, No. 2, 1981, pp. 172–179.

[7]Weir, L. J., Reddy, D. R., and Rupp, G. D., "Mach 5 Inlet CFD and Experimental Results," AIAA Paper 89-2355, July 1989.

[8]Carter, T. D., and Spong, E. D., "High Speed Inlet Investigation. Vol. I Description of Program and Results; Vol. II Data Summary," Air Force Flight Dynamics Lab., AFFDL-TR-77-105, Wright-Patterson AFB, OH, Nov. 1977.

[9]Strike, W. T., and Rippy, J., "Influence of Suction on the Interaction of an Oblique Shock with a Turbulent Boundary Layer at Mach 3," Arnold Engineering Development Center, AEDC-TN-61-129, Tullahoma, TN, Oct. 1961.

[10]Seebaugh, W., and Childs, M., "Conical Shock Wave Boundary-Layer Interaction Including Suction Effects," *Journal of Aircraft*, Vol. 7, No. 4, 1970, pp. 334–340.

[11]Benhachmi, D., Greber, I., and Hingst, W., "Experimental and Numerical Investigation of an Oblique Shock-Wave/Turbulent Boundary Layer Interaction with Continuous Suction," AIAA Paper 89-0357, Jan. 1989.

[12]Gubbison, R. W., Meleason, E. T., and Johnson, D. F., "Performance Characteristics from Mach 2.58 to 1.98 of an Axisymmetric Mixed Compression Inlet System with 60 Percent Internal Contraction," NASA TM X-1739, Feb. 1969.

[13]Fukuda, M. K., Hingst, W. G., and Reshotko, E., "Control of

Shock Boundary Layer Interactions by Bleed in Mixed Compression Inlets," NASA CR 2595, 1975.

[14]Wong, W. F., "The Application of Boundary Layer Suction to Suppress Strong Shock-Induced Separation in Supersonic Inlets," AIAA Paper 74-1063, Oct. 1974.

[15]Beam, R., and Warming, R., "An Implicit Factored Scheme for the Compressible Navier-Stokes Equations," *AIAA Journal*, Vol. 16, No. 4, 1978, pp. 393–402.

[16]Visbal, M., and Shang, J., "Comparative Study Between Two Navier-Stokes Algorithms for Transonic Airfoils," *AIAA Journal*, Vol. 24, No. 4, 1986, pp. 599–606.

[17]Visbal, M. R., "Calculation of Viscous Transonic Flows About a Supercritical Airfoil," Air Force Wright Aeronautical Labs., AFWAL-TR-86-3013, Wright-Patterson AFB, OH, July 1986.

[18]Hamed, A., and Lehnig, T., "An Investigation of Oblique Shock/Boundary Layer Interaction," *Journal of Propulsion and Power*, Vol. 8, No. 2, 1992, pp. 418–424.

[19]Hakkinen, R. J., Greber, I., Trilling, L., and Aberbanel, S. S., "The Interaction of an Oblique Shock Wave with a Laminar Boundary Layer," NASA Memo 2-18-58W, March 1959.